Published in final edited form as:
Curr Opin Colloid Interface Sci. 2011 June 1; 16(3): 203–214. doi:10.1016/j.cocis.2010.12.004.

Novel Methods of Enhanced Retention in and Rapid, Targeted Release from Liposomes

Joseph A. Zasadzinski[*],
Department of Chemical Engineering and Materials Science, University of Minnesota, Minneapolis, Minnesota 55455

Benjamin Wong,
Department of Chemical Engineering, University of California, Santa Barbara, California 93106

Natalie Forbes,
Department of Chemical Engineering, University of California, Santa Barbara, California 93106

Gary Braun, and
Department of Chemistry, University of California, Santa Barbara, California 93106

Guohui Wu
Department of Chemical Engineering, University of California, Santa Barbara, California 93106

Abstract

Liposomes are single bilayer capsules with distinct interior compartments in which hydrophilic drugs, imaging agents, diagnostics, etc. can be sequestered from the exterior environment. The polar parts of the individual lipids face the water compartments, while the hydrophobic parts of the lipid provide a barrier in which hydrophilic or charged molecules are poorly soluble. Hydrophobic molecules can be dissolved within the bilayer. The bilayers are typically from 3 – 6 nm thick and the liposome can range from about 50 nm - 50 microns in diameter. The question asked in this review is if any one bilayer, regardless of its composition, can provide the extended drug retention, long lifetime in the circulation, active targeting to specific tissues and rapid and controllable drug release at the site of interest. As an alternative, we review methods of self-assembling multicompartment lipid structures that provide enhanced drug retention in physiological environments. We also review methods of externally targeting and triggering drug release via the near infrared heating of gold nanoshells attached to or encapsulated within bilayer vesicles.

Keywords

Surface plasmon resonance; hollow gold nanoshells; cancer chemotherapy; phospholipids; sphingomyelins; siRNA delivery; doxorubicin delivery

[*]To whom correspondence should be addressed zasad008@umn.edu or gorilla@engineering.ucsb.edu, Phone: 805-893-4769, FAX: 805-893-4731.

Major Recent Advances

Simple unilamellar liposomes have become the building blocks of increasingly complex nanostructures proposed to address the implications of harsh, physiological environments on lifetime in the bloodstream, drug retention, targeting to specific sites, and spatially and temporally controlled release rates. Multiple levels of encapsulation within layers of polymer (1) or lipid (2,3) can prolong drug retention by orders of magnitude over unilamellar liposomes of the same composition. Adsorbing, tethering, or encapsulating near infrared light adsorbing gold nanoparticles (4–8) provides new targeting and release mechanisms with physiologically friendly near infrared light, while retaining the advantages of liposome biocompatibility and biodistribution. Gold nanoparticles can also be used to rupture endosomal membranes within living cells to enhance transfection without damaging the cells themselves as a novel way of *in vivo* transfection for siRNA induced gene silencing (9,10).

1. Introduction

It is often difficult to maintain drug levels within the concentration range necessary to avoid toxicity while maintaining efficacy (11,12) using systemic drug delivery. This therapeutic window can be expanded by altering drug biodistribution by using nanoscale delivery systems to maximize concentration at the disease site while decreasing toxicity by lowering drug concentrations elsewhere in the body. Liposomes and other lipid-based drug carriers were among the first methods used to sequester toxic drugs to provide significant advantages by altering drug biodistribution, enhancing efficacy while minimizing damage to healthy organs and tissues.

Liposomes (or vesicles) are spheroidal closed lipid bilayer structures with one or more distinct internal aqueous compartments. Small (< 400 nm), usually unilamellar liposomes can carry hydrophilic agents within these aqueous compartments, such as the doxorubicin in Doxil, an FDA approved liposomal delivery system for systemic delivery of cancer chemotherapy, or hydrophobic agents within the bilayers, such as amphotericin B, an anti-fungal agent in AmBisome (13). Complex structures, often called lipoplexes, similar to liposomes, can self-assemble from cationic lipids, or mixtures of cationic and neutral lipids such as Lipofectamine (Invitrogen. Carlesbad, CA), and anionic DNA or RNA, and are used to transfect cells in culture. Uni- and multilamellar liposomes also show great promise as delivery vehicles for a variety of cosmeticeuticals, pharmaceuticals, diagnostics and imaging agents. The lipid bilayer surface is inherently biocompatible and can be functionalized with specific ligands, antibodies or polymers to improve the residence time in the circulation or target specific sites. Larger (10 – 100 μm), multicompartment lipid carriers have been used as slow-release depots for drugs such as cytarabine in the clinically approved Depocyt; the larger size helps to localize the carrier to the site of injection (14).

Nanoscale lipid delivery vehicles can take advantage of the enhanced permeability and retention (EPR) effect, which is a passive targeting mechanism that exploits the rapid angiogenesis (formation of new blood vessels from existing ones) of tumor and inflammation sites (12,15,16). The blood vessels associated with tumors are often leaky and dysfunctional, with poor lymphatic drainage. Whereas free drugs diffuse non-specifically, a nanocarrier can escape preferentially through the leaky vessels surrounding a tumor, which is the first step of the EPR effect. The ineffective lymphatic drainage in tumors helps retain liposomes that do extravasate and allows the liposomes to accumulate in the neighborhood of the tumor. The threshold liposome size for extravasation into tumors is from 400 – 500 nm, but smaller nanoparticles with diameters less than 200 nm are believed to be more effective (11,15,16). The minimum size for a nanocarrier is about 5 nm, which is the kidney

filtration cut off size (17). Passively targeted liposomes reached clinical trials in the mid-1980s, and were approved for clinical use in the mid-1990s (11,15).

However, the EPR effect varies from tumor to tumor, especially in solid tumors (12,16). Drugs only penetrate a few cell diameters into the extravascular tumor tissue from blood vessels due to the poor perfusion of the blood vessels in the growing tumor (16,18), resulting in a heterogeneous distribution of therapeutic agents. The high interstitial pressure due to the dysfunctional lymphatic drainage causes fluid to flow out of the tumor, working against diffusion of drugs (16,18); hence, the same factors that provide the EPR effect that retains nanoparticles in the tumor can work against a therapeutic distribution of drugs released from those nanoparticles. Small molecules, such as doxorubicin, are not able to diffuse more than 40 – 50 microns from the vasculature, leaving many cells exposed to sublethal doses that can contribute to the development of drug resistance (15). New tumor-penetrating peptides may enhance the permeability of solid tumors to nanoparticles, including liposomes, thus increasing the local concentration of both liposomes and drugs within the tumor (12). Controlling the rate of drug release from liposome or other depots might also provide better penetration in the face of high interstitial pressure and convective flow (16,18).

Active targeting can be accomplished by conjugating liposomes containing chemotherapeutics with molecules that bind to antigens or receptors on the target cells (6,12,16,19). Optimally bound liposomes can be internalized before the drug is released, which minimizes toxicity to other cells. The efficacy of such targeting is determined primarily by the selectivity to receptors that are uniquely expressed on the target cell surface. In practice, a surface marker must be significantly over-expressed on target cells relative to normal cells, as the number of normal cells usually dwarfs the number of target cells in the body. Each new target tissue requires identifying the appropriate receptors and developing new ligands to target them (6,12,16). It is also possible to facilitate over-expression of a specific receptor on tumors using pretreatments. Park et al (6) have used gold nanorod-induced local hyperthermia to up-regulate receptors in heated tumors, which could then be recognized by liposomes with ligands specific to those receptors (Figure 1). The combination therapy was more effective in tumor suppression than either nanoparticles or liposomes alone.

While high binding affinities usually increase targeting efficacy, there is evidence that this affinity can lead to “binding-site barriers” where the tightly bound nanocarriers prevent drug penetration into the tissue (15). High selectivity can also have unexpected consequences when the target has multiple roles or locations on different cell types (18). A second limitation is the rapid development of resistance, which is more likely if a single molecular receptor is being targeted with high selectivity. For example, Gleevec (imatinib mesylate) has become the treatment of choice for chronic myelogenous leukemia and gastrointestinal stromal tumors, but in many cases becomes ineffective after prolonged use. Imatinib targets a specific tyrosine kinase that can mutate, which makes it no longer sensitive to the imatinib. While this confirms the high selectivity of imatinib toward a specific molecule, it reflects an important limitation to therapies based on highly specific targeting to a single receptor. Any variations or mutations in the receptor make the targeting less effective, resulting in drug resistance. A better approach may be to develop a bank of ligands toward a family of receptors. However, this is a very costly strategy and may not always prove effective (18).

Both active and passive liposome targeting require sufficient circulation times in the bloodstream to allow the liposomes to accumulate in the target tissue. Short *in vivo* half-life can be an advantage in imaging as it eliminates the background caused by unbound probe. However, longer circulation times are necessary when the therapeutic target is outside the vasculature and the liposomes must take advantage of the EPR effect. The half-life of a drug

depends either on the rate of elimination into the urine (small molecules) or for nanocarriers, uptake by the reticuloendothelial system (RES) (15,16). The RES is a part of the immune system that consists of phagocytic cells such as monocytes and macrophages that accumulate in lymph nodes and the spleen (20). The Kupffer cells of the liver are also part of the RES. The RES eliminates foreign particles from the circulation and limits the amount of nanocarriers that can reach a specific target. Opsonization, or the coating of nanoparticles with plasma proteins that mediates binding to the Kupffer cell receptors in the liver is thought to initiate the removal of nanoparticles from the circulation, but the molecular mechanisms are not well understood (15,16). Anionic or neutral liposomes less than 200 nm in size that have been coated with polyethylene glycol (PEG) or hyaluronan extend circulation times in mice (15,16), although RES removal is only delayed, not prevented. There is still disagreement if the main function of PEG-lipid is to reduce liposome aggregation via a classic polymer steric repulsion effect or to reduce plasma protein adsorption, thereby preventing opsonization and removal by the RES system (21). However, recent work has shown that there is little variation in total protein adsorption or the species of protein adsorbed to liposomes with the surface coverage of PEG-lipid, or by the PEG molecular weight (21). Increasing the density of the PEG chains on solid nanoparticles from the “mushroom” to the “brush” configuration switches complement activation from C1q–dependent classical to the lectin pathway, and reduced the level of complement activation products (22,23). However, liposomes can be destabilized by increased PEG-lipid concentrations and become leaky or even change structure (24). An alternate explanation of the effect is that the PEG-lipid increases the potential for hydrogen bonding with the surrounding water; liposomes with 10 – 30 mole% of an anionic, glycerol-modified phospholipid (1,2-dipalmitoyl-sn-glycero-3-phosphoglyceroglycerol) showed enhanced circulation times (25). A better understanding of the clearance mechanisms and means of avoiding clearance is necessary to take optimal advantage of nanocarriers for intravenous drug delivery.

Up to now, the most significant successes of molecularly targeted agents have been against leukemias and lymphomas, with less success against most adult epithelial cancers (18). Solid tumors are heterogeneous and are made up of multiple cell types in different environments, ranging from almost normal for those cells in the vicinity of the vasculature, to necrotic in regions farther from the vasculature. In between, the cells can be highly stressed by hypoxia, acidity and high interstitial pressure, which make them more or less responsive to many drugs and targeted carriers. It is unlikely that all cell types in a solid tumor will be equally responsive to any one class of highly targeted anticancer agents, requiring a multipronged, multistep approach (18) including multifunctional carriers capable of delivery a variety of drugs at various rates.

2. Drug Retention - Delivering Magic Bullets or Empty Promises

The basic liposome structure used for drug delivery has not undergone significant alteration since its introduction more than 40 years ago. Conventional unilamellar liposomes used in drug delivery have a single, usually spherical compartment, delimited by a single bilayer membrane, which mimics the single compartment structure of the prokaryote cell (for an extensive recent review of liposome fabrication and applications, see Volumes 464 and 465 of *Methods in Enzymology*, edited by N. Düzgünes (2009)). This bilayer defines the interior space, regulates release of the liposome contents, and protects the liposome and its contents from the environment. Sizes of unilamellar liposomes can vary from 50 nm – 50 microns depending on the method of preparation; the smaller liposomes are typically prepared by extrusion through filters of the appropriate pore size or by sonication of larger liposomes; the larger liposomes are prepared by a variety of techniques including simple hydration of lipids dried from solvents (5). With few exceptions (2,26,27), essentially all of the literature

on liposomes involves modifying the chemical and physical properties of this single bilayer to optimize these tasks. However, it is difficult for a given bilayer to combine the necessary physical integrity and drug retention in circulation (to maximize drug accumulation at the disease site) with controllable contents release at the disease site (to effect therapy and minimize drug resistance). Despite 40 years of extensive research, only doxorubicin (or the chemically similar daunorubicin) for chemotherapy and amphotericin B in anti-fungal preparations are clinically available in intravenous liposome formulations. (The clinically approved Depocyt is cytarabine encapsulated in multicompartment lipid bilayer "foam" particles of > 10 microns in diameter used as a drug depot, not as a drug delivery vehicle (14).) Doxorubicin forms precipitates within liposomes when loaded with a ammonium sulfate gradient which accounts for the slow release of the drug *in vivo* (28). In fact, much of the benefit of liposomal doxorubicin is the reduction in drug-related toxicity, as its therapeutic activity is reduced despite its efficient delivery to tumors due to slow release from the liposome carriers.

On the other hand, many other drugs, such as the antibiotic ciprofloxacin and the chemotherapy agents vinorelbine, vinblastine and vincristine, leak out too rapidly from phospholipid liposomes in a physiological environment (29), which severely limits the efficacy of unilamellar vesicles as universal drug carriers. While coating the exterior of vesicles with lipids functionalized with polyethylene glycol (PEG) (24) extends *in vivo* circulation times to 24 – 48 hours, PEG-lipids actually increase liposome permeability and do not enhance drug retention (24). It is difficult for any single membrane to combine the necessary physical integrity and drug retention in circulation (to maximize drug accumulation at the disease site) with rapid contents release at the disease site (to effect therapy and minimize drug resistance).

Optimizing the bilayer composition to maximize liposome retention depends on a variety of choices, including lipid headgroup, saturation of the lipid alkyl chains, and the addition of cholesterol (29,30). Long chain (≥ 16 carbons long for phosphatidylcholines), saturated lipids form an ordered, semi-crystalline gel phase (L_β phase if the alkane chains are normal to the bilayer or $L_{\beta'}$ phase if the chains are tilted) that melts to form a more fluid, L_α liquid crystalline phase. Permeation is much slower in the gel phase, leading to better retention of small molecules within the liposome (2,30). Drummond et al. (30) have recently reviewed the effects of lipid composition, liposome size, and the various agents used to complex or load drugs into liposomes on drug retention within single bilayer liposomes. While many of these modifications decrease bilayer permeability by orders of magnitude *in saline*, the differences in contents retention with bilayer composition are less pronounced in serum and other physiological environments (2,29–31).

This is because drug release occurs by quite different mechanisms in physiological fluids than in saline or buffer (2,21,30,32–36). In physiological media, phospholipids and/or cholesterol can be removed from liposomes by plasma high density lipoproteins (HDL), leading to the formation of pores in the bilayer and release of the liposome contents (32,36). Lipases, such as PLA_2, can bind to the liposome and selectively cleave the ester linkage of phospholipids molecules, leaving behind a lysophospholipid and a fatty acid (2); at sufficiently high lysolipid/fatty acid fractions, the liposomes are destabilized. Increasing the mole fraction of cholesterol to 30 mole% or higher eliminates the thermotropic phase transition from the gel to liquid crystalline phase in phospholipid bilayers, decreases the permeability of the bilayer, and inhibits the insertion of hydrophobic enzymes such as lipases and proteins into the bilayer (34). Liposomes containing cholesterol are more stable and less leaky than those without cholesterol; essentially all liposomes used in drug delivery contain a substantial fraction of cholesterol (30).

However, when liposomes composed of cholesterol and phospholipids are placed in contact with biomembranes and proteins, cholesterol can be removed from the liposome bilayer (34,36,37). Removing cholesterol from the liposome destabilizes the liposome, and leaves it susceptible to protein insertion, lipase attack, etc. The rate-limiting step in removing cholesterol is believed to be the solubility of cholesterol in the aqueous phase relative to the bilayer (34,36,37). This aqueous diffusion pathway is bidirectional; cholesterol can be exchanged between liposomes, cell plasma membranes and HDL. The direction of net cholesterol transport is determined by the cholesterol concentration gradient as reflected by the cholesterol/phospholipid ratios in the donor and acceptor particles (36,37). Szoka and coworkers have tried to minimize this cholesterol exchange by chemically coupling the cholesterol to a phospholipid head group, which appears to slow cholesterol exchange from the liposome to other biomembranes, likely by decreasing the water solubility of the cholesterol (34).

Replacing phospholipids by sphingomyelin can also increase drug retention, particularly in the presence of cholesterol (29,33). The reduced permeability of the membrane is believed to result from hydrogen bonding between the amide nitrogen of sphingomyelin and the hydroxyl group of cholesterol (30). In addition, the amide linkage in the sphingomyelin backbone is less sensitive to pH-dependent hydrolysis than the ester linkages of phospholipids, which can also contribute to the enhanced drug retention by enhancing the chemical stability of the bilayer. As is the case for phospholipids, fully saturated dihydrosphingomyelin increases liposome stability and drug retention compared to unsaturated sphingomyelins (33). However, the PEG-lipids used to inhibit aggregation and opsonization destabilize sphingomyelin-cholesterol liposomes, which makes increasing circulation times problematic (33).

2.1 Structural Solutions to Increased Contents Retention

Modifying the basic structure of the liposome has received much less attention than changes in the bilayer composition or methods of loading drugs within the liposome. One fundamental difficulty with phospholipid and sphingolipid unilamellar liposomes is that they are thermodynamically unstable against aggregation and fusion; the multilayered lamellar phase is the stable phase under most conditions (38). Fusion into larger structures causes the contents of the liposomes to leak and the average size increase, making EPR less effective. The actual benefit of incorporating PEG-lipids into the bilayer may be to slow fusion due to the steric repulsion induced by the polymer (21,24). Even relatively small surface coverages of PEG (~ 20%) provide significant decrease in clearance from the circulation (21); these small surface coverages are sufficient to provide steric stabilization against aggregation. However, these same surface coverages do not seem to prevent protein adsorption. Unfortunately, PEG-lipids can partition to other membranes or micelles with time after dilution *in vivo* or *in vitro*, or when placed into solution with other bilayers or membranes to which the PEG-lipids could insert. This decreases the steric repulsion needed to stabilize liposomes against fusion with time, which may be why liposomes are eventually cleared from the circulation (21,24). This decrease in surface coverage cannot be extended just by increasing the initial PEG-lipid fraction in the liposome; sufficiently high PEG-lipid fractions disrupt the bilayer structure, resulting in the formation of bilayer discs and micelles (21,24).

Protection against fusion can also be obtained by adsorbing charged polymer nanoparticles to zwitterionic liposome bilayers (39). The nanoparticles provide both steric and electrostatic modes of stabilization against liposome fusion (40), especially in low ionic strength media. However, the nanoparticles lose effectiveness in higher ionic strength media as the electrostatic interactions are screened (40), and hence, this method would not be as useful *in vivo*. As is the case for PEG-lipids, adsorbing charged nanoparticles to neutral

bilayer membranes via a dipole attraction can induce changes in the bilayer organization and structure that need to be taken into consideration when designing composite drug delivery vehicles (39,40). Stronger interactions between neutral lipid bilayers and strongly hydrophilic silica nanoparticles can disrupt bilayers and cause the nanoparticles to be engulfed by liposomes (41). It is important to remember that bilayer organization and self-assembly are governed by weak interactions between lipid molecules that can be altered by even weak interactions with other particles or surfaces (41). As of yet, there have been no studies to determine the circulation lifetimes of these nanoparticle-stabilized liposomes.

Stronger binding of charged nanoparticles to liposomes can be accomplished by adding the oppositely charged lipid to the bilayer membrane (31). 10 – 30 nm diameter gold nanoparticles, which are anionic, can be adsorbed to liposomes that contain various fractions of cationic lipids (31). Depending on the ratio of gold nanoparticles to liposomes, the liposomes can be cross-linked by the nanoparticles to form small aggregates of liposomes and nanoparticles (31). Aggregating the gold nanoparticles red-shifts their adsorption spectra from about 520 nm for single gold nanoparticles to 650 – 800 nm for larger aggregates (31). This red-shift to higher wavelength puts the adsorption into the “near infrared window”, in which there is minimal adsorption by blood, tissue, and other biological molecules (4,5). If higher ratios of gold nanoparticles are used relative to the liposomes, each liposome is covered by nanoparticles, and the nanoparticles stabilize the liposomes against fusion (41).

Directly plating gold onto a liposome template has also been suggested as a method of improving drug retention and liposome stability (7,42), as well as providing a mechanism for light-triggered release. Conventional phospholipid liposomes are coated with gold by adding ascorbic acid to a liposome solution containing chloroauric acid, which reduces the gold salt to metallic gold (7,43). The reaction can be followed by the evolution of the adsorption spectra, which shows a maximum in the near infrared region as the adsorption increases. When gold is produced in this fashion, small gold crystallites, 4 – 8 nm in diameter, precipitate preferentially on the liposome surface. Depending on the gold to liposome ratio, the crystallites can eventually fuse and form a discontinuous shell. Dye contained in these gold covered liposomes is released similarly to uncoated liposomes in a temperature-dependent fashion (7). Better drug retention is claimed if the gold shell can be made continuous by first precipitating a layer of poly-L-histidine (PLH) onto a anionic liposome template (42). The PLH layer is capable of chelating metal ions, which is believed to assist in the formation of a continuous gold shell, rather than small gold clusters (42). TEM images of dried samples of the gold covered liposomes showed that the sizes were quite different than the original liposome template, with diameters as small as 10 nm, so it appears that the original, 100 nm liposome template is lost during the growth process. However, care must be taken in characterizing liposome structure from dried samples as the liposome structure is unstable without water present; cryogenic TEM methods such as freeze-fracture (2,44) or cryo-TEM are necessary to preserve the original structure for imaging (4,5).

A variation on these techniques is to precipitate polyelectrolytes (1,42,45,46) onto a liposome template. Successive adsorption of cationic and anionic polymers to a suitably charged colloidal substrate is known as layer-by-layer (LBL) deposition (1,42,45,46). Caruso and coworkers have made “caposomes,” which are cell mimics with a large, but controllable number of lipid compartments encapsulated within a polymer scaffold (Figure 2). First, an anionic silica particle is coated by a cationic polylysine layer (PLL). Conventional small, unilamellar liposomes, which can be formed from zwitterionic or negatively charged lipids are then mixed with the polylysine-coated silica particles. The liposomes bind to the PLL coated silica and are subsequently covered by a layer of cholesterol-modified polylysine to anchor the polymer layer to the liposomes. A second

layer of liposomes can then be added to the structure, followed by a second PLL coating. Alternately, spacer polymer layers of anionic poly (methylmethacrylic acid)-co-cholesteryl methacrylate (PMAC) can be added between the liposome layers. Finally, the assembly is sealed by the sequential adsorption of poly(N-vinyl) pyrrolidone and thiol-functionalized poly(methacrylic acid); (PVP-$PMA_{SH})_5$-PVP). The thiols in the outer layer can be cross-linked, and the silica core etched to form the capsosome (1). These novel structures are extremely robust due to the multiple polymer layers and cross-linking and can have thousands of internal compartments. The overall structure is 5 – 10 microns in size and would not be appropriate for use in the circulation, but rather as a drug depot, although the toxicity of these polymers and their metabolites is not yet known.

A multicompartment structure based on liposomes within liposomes or “vesosome” (Figure 3) (2,3) can also be constructed using basic self-assembly. Eukaryotes developed this nested bilayer structure as a successful alternative to optimizing the chemistry and physics of a single bilayer; each compartment has its own distinct bilayer membrane which separates different functions while protecting the internal contents from the environment (2,3). The inner compartments can encapsulate multiple drugs (to deliver drug cocktails or have different bilayer compositions to optimize release or do various chemical reactions (3). In addition, while it is difficult to encapsulate anything larger than molecular solutions by conventional vesicle self-assembly, the vesosome construction process lends itself to trapping colloidal particles (Figure 5) and biological macromolecules (2).

To encapsulate liposome suspensions within another bilayer membrane, a way of opening and closing one population of bilayers that does not compromise other liposomes is necessary. Most bilayers, regardless of composition, form closed spherical structures in aqueous solution to shield the hydrophobic interior of the bilayer from the exterior solution, at the cost of bending the bilayer into the spherical form. Bilayers in the liquid crystalline L_α or the gel phase L_β or $L_{\beta'}$ phases have sufficiently small bending moduli that closed liposomes as small as 50 nm in diameter are stable. However, below the gel-liquid crystalline transition temperature, T_m, a number of saturated phospholipids that form the tilted $L_{\beta'}$ phase form L_{bI} or “interdigidated” phases on addition of ethanol and other short-chain alcohols. Lipids that form a tilted $L_{\beta'}$ phase do so because the frozen, all-trans acyl chains of the lipids must tilt to accommodate the larger interfacial area required by the hydrophilic head groups. Saturated phosphatidylcholines and phosphatidylglycerols, with large head groups, form tilted $L_{\beta'}$ phases below T_m, while phosphatidylethanolamines, with small head groups, form untilted L_β phases. Adding ethanol to PC or PG liposomes in the $L_{\beta'}$ phase causes the headgroup area to increase due to the intercalation of the ethanol into the headgroup region. At about 3 molar ethanol, the area required by the headgroups can no longer by accommodated by increasing the chain tilt, and the all-trans acyl chains of the opposing monolayers interdigitate (2). This interdigitation increases the membrane rigidity dramatically, and the increased curvature energy destabilizes small vesicles and leads to the formation of open bilayer sheets in solution. These sheets are stable as long as the temperature is held below T_m and the acyl chains are frozen. Heating above T_m causes the acyl chains to melt and the membrane reverts to a disordered, L_α bilayer phase. The reduced bending rigidity of the L_α phase allows the bilayers to close; in the process, small vesicles, gold nanoshells, colloidal particles, essentially anything of nanometer dimensions in the original suspension (2,4) can be encapsulated as shown in Fig. 3.

Having two or more bilayers between the environment and the drug contents can make a significant difference in drug retention in physiological environments. Figure 4a shows that the additional bilayer barrier in the vesosome effectively eliminates drug release caused by exposure to phospholipase A_2 (PLA_2). Carboxyfluorescein dye release from unilamellar vesicles DPPC was rapid after exposure to varying amounts of porcine pancreas PLA_2 at 37°

C (closed symbols), with complete release within 4– 8 hours. Essentially no release beyond background is induced by PLA_2 from vesosomes over 20 hours (open symbols). This indicates that the PLA_2 cannot traverse the exterior bilayer of the vesosome to degrade the internal vesicles during the time of the experiment. While PLA_2 increases the permeability of the small molecule CF (molecular mass of 376 Da) from unilamellar vesicles, apparently it takes much longer for PLA_2 (molecular mass of 14 kDa) itself to cross the exterior lipid bilayer of the vesosome. The exterior membrane also protects the interior vesicles from binding to streptavidin when the interior lipid bilayers are decorated with biotinated lipids (2). Both the inner and outer vesosome bilayers are composed of DPPC, as are the unilamellar vesicles, hence, this dramatic increase in retention is due solely to the liposome within liposome structure.

Figure 4b shows a similar protective effect of the exterior membrane in fetal bovine serum. The vesosome structure extends the half-life for release from vesosomes in serum to more than 50 hours (from about 2 hours for unilamellar vesicles of DPPC (2)), and there appears to be a delay in release for ~ 10 hours before any significant amount of CF is released. The serum components responsible for degrading the bilayers and increasing permeability were effectively shielded from the interior compartments for this initial period. The additional bilayer membrane provides a physical barrier to biological macromolecules and high-density lipoproteins; it takes much longer for these high molecular weight structures to traverse the bilayer than small molecular weight drugs or dyes. The lack of direct interaction between the interior compartment and the external medium efficiently delays CF leakage; the structure provides the additional retention time. In addition to the structural barrier, even greater retention may be possible by encapsulating interior compartments with different composition. For example, if sphingomyelin-cholesterol inner vesicles were used, they would be resistant to phospholipases and also provide an additional permeability decrease due to the decreased sensitivity to pH-dependent hydrolysis. PEG-lipids can be incorporated in the outer, DPPC bilayer to provide steric stabilization, (which is not possible for sphingomyelin liposomes (33)) providing a half-life in the mouse circulation of about 2–3 hours (47).

3. Controlling and Targeting Liposome Contents Release

Enhanced drug retention has a cost; the therapeutic activity of liposomal doxorubicin is reduced due to slow release from the liposome carriers, although liposome delivery reduces drug-related toxicity (19). Reducing the rate of drug release may cause tumor cells to be exposed to sublethal doses that could contribute to the development of drug resistance or accumulation of the drug that lead to side effects such as palmoplantar erythrodysesthesia (hand-foot) syndrome (15,48,49). While the basis of cancer drug resistance is complex, the over-expression of MDR transporters, which are integral membrane proteins, likely plays a role. MDR transporters actively pump chemotherapeutic drugs out of cells and reduce the intracellular drug concentration below the lethal threshold. Hence, if the rate of drug release from a carrier is too slow, only drug-sensitive cells that do not express MDR are killed, leaving behind a population resistant to the rate of drug release (15). Chemotherapy may fail because residual drug-resistant cells eventually dominate the tumor population. Therefore, one of the parallel challenges for liposome and other nanocarrier development is to devise ways of optimizing the rate of encapsulated drug release, with both spatial and temporal control (5,8,31,46,50,51). External signals such as ultrasound (52) and visible light (53,54) have been used to induce contents release from liposomes, but these methods are limited to surface accessible areas such as the eye and skin. For delivery to deeper tissues, other strategies have emerged, including liposomes sensitized to general hyperthermia (25,51,55), and pH or enzymatically triggered liposomes (56). However, it is often difficult to

incorporate a destabilizing agent into the liposome membrane to promote release without affecting long-term stability and drug retention in the circulation.

A new, widely adaptable and physiologically friendly method of triggering rapid liposome contents release is to incorporate gold nanoparticles into the liposome, or attach nanoparticles to the liposome membrane (4,5,7,31). When gold nanoparticles are exposed to laser light of the appropriate wavelength, the particles strongly adsorb the light and rapidly and efficiently convert the light energy into heat (4,5,7–9,50,57–59). By adjusting the size and shape of the nanoparticles (length to diameter ratio for nanorods (50,59), shell thickness to diameter for nanoshells (57)), the frequency of the surface plasmon resonance (SPR) can be tuned to preferentially adsorb light from 650 – 900 nm, the so-called near infrared (NIR) window. The great advantage of this window is that tissue, blood, etc are relatively transparent to NIR light, allowing penetration depths of several centimeters (50,59). Silica core/gold nanoshells (57), aggregates of solid gold nanoparticles (7,31), gold nanorods (6), and hollow gold nanoshells (HGN) or nanocages (4,5,9,10,27,43,58) are all effective at absorbing NIR light and converting this energy into heat. Gold nanoshells and nanorods illuminated with NIR light have been successfully used to non-invasively heat and eradicate diseased cells and tissues both *in vivo* and *in vitro* (6,9,10,27,31,46,50,57).

The SPR is caused by the oscillating electromagnetic field of light which induces a coherent oscillation in the conduction band electrons of the nanoparticles (50,57). This oscillation induces a charge separation between the free electrons and the ionic metal core, which in turn causes a restoring Coulomb force that makes the electrons oscillate back and forth on the particle surface. This SPR oscillation induces a strong adsorption of light of specific frequencies which depends on the shape, size and composition of the nanoparticle (50). Nanoparticle adsorption can be 5–6 orders of magnitude larger than that of dye molecules, which have also been used to sensitize liposomes (50).

HGN that adsorb strongly in the NIR are made by galvanic exchange of gold with a silver template (43,60); the silver template is oxidized away as soluble ionic silver as the gold is reduced to metal; a hollow shell of gold precipitates on the silver template. The ratio of shell thickness to shell diameter determines the surface plasmon resonance, and hence the optimal wavelength for adsorption (43,57,59). The shell diameter is set by the size of the silver template, while the shell thickness can be tuned by varying the quantity of gold salt used in the reaction (9,43). The synthesis of gold nanorods and nanoshells can be found in recent reviews (5,43,50,57,59); a variety of shapes and sizes are available commercially. For NIR applications, HGN range from 20 – 50 nm in diameter, with 2 – 5 nm thick shells (Fig. 5) (4,5,9,43). HGN can be encapsulated within unilamellar DPPC liposomes using the same interdigitated sheet method used to make the vesosome (Figure 5a) (4). Alternately, there are a variety of thiol-PEG-lipid linkers that can be used to tether HGN to the liposome bilayer (Figure 5b). Finally, HGN can simply be mixed with liposomes (Figure 5c). It is found that the closer the HGN is to the liposome membrane, the more efficient is the contents release (4) upon pulsed laser irradiation.

The lifetime and intensity of the laser irradiation used induce widely different temperature responses in the gold nanostructures. Continuous wave, low intensity excitation is used to heat both the nanoshells and the surrounding medium (7,31,57) by a few to tens of degrees, depending on the length of irradiation time and the intensity of the light flux. The nanoshells never reach temperatures significantly different than the surrounding fluid. On the other hand, if the laser pulse duration is shorter than the time necessary for the gold nanoparticle to thermally equilibrate with its surroundings, all of the light energy goes into heating the nanoparticle (4,5,9,43,61). For nanometer-sized gold particles, thermal equilibration with the environment occurs in 10 – 100 nanoseconds; which is long compared to the femto- to nano-

second pulses possible with current lasers (43,50,61). The nanoparticle temperature can reach > 1000° C (43,61), sufficient to melt the gold nanoparticles, before the energy can be transferred to the surrounding liquid (43,50). The conversion of the optical energy into heat is so fast (nanoseconds) that thermal energy dissipation to the surrounding fluids occurs *after* the HGN reaches its maximum temperature (5,50).

Figure 6a shows a fluorescence image of a liposome containing fluorescent allophycocyanin (APC) protein and 80 nm solid gold nanoparticles (adsorption maxima at 532 nm) attached to an anionic glass surface (8). Fig. 7b shows that only 10 nsec after irradiation with a 0.5 nsec light pulse, a large, asymmetric vapor bubble was formed, with dimensions growing much larger than the liposome. The rapid expansion and collapse of these bubbles causes transient liposome rupture and contents release (4, 5, 8, 61). The rapid bubble expansion and collapse induces mechanical stresses in the surrounding fluid, which can tear lipid membranes apart, thereby releasing the contents of liposomes (4). Within milliseconds after irradiation, the APC was released from the liposome (7c). The solution re-achieves equilibrium less than a millisecond after the initial laser pulse (4, 8). Depending on the laser power and the pulse repetition rate, the average solution temperature is increased by no more than a few degrees (43). There is a minimum energy threshold for drug release and a characteristic acoustic response of the solution on irradiation (4, 5), similar to sonication-induced cavitation. Hence, irradiation of the HGN with pulsed NIR light produces the same effects on the liposome membrane as those induced by ultrasound-induced cavitation (4). Sonication is a commonly used method to create small, unilamellar vesicles from a lamellar dispersion and is well known to disrupt bilayer membranes.

This photo-activated release also provides a secondary targeting mechanism that could be used to increase selectivity for both passively (EPR mechanism) and actively (peptide or antibody) targeted liposomes. Release would be localized to the focus of the laser light source, and fast and near complete drug release could be achieved within seconds of irradiation (4,5,8) with minimal (whatever residual permeation would occur without irradiation) elsewhere. Gold is generally considered to be inert and biocompatible, especially in comparison to many of the dyes used to photosensitize liposomes. While the actual depth of penetration depends on tissue type and scattering, NIR can penetrate several centimeters inside the body, which makes it much more appropriate for drug release than UV or visible light, which penetrates fractions of a millimeter. High localized drug concentrations can prevent the development of drug resistance, and the timing of the drug release can be determined independently of the properties of the nanocarrier. In addition, HGN-induced liposome disruption may be used to induce rapid diffusional mixing to permit the study of fast chemical kinetics in nanoenvironments mimicking cell membranes (3). An additional benefit of HGN-induced disruption is that the heat generation is extremely localized; endosomes can be disrupted without otherwise damaging the cell (9).

3.1 Disrupting Bilayers In Vivo with Gold Nanoshells

In vivo delivery of DNA, siRNA and oligonucleotides remains difficult as no suitable non-viral vector has yet been developed that is biocompatible, circulates efficiently in the bloodstream, is readily targeted to the appropriate site, and efficiently enters the cell cytoplasm or nucleus (9–11,62,63). Oligonucleotides cannot be injected directly into the bloodstream, or even into serum-containing cell culture media, due to rapid degradation by nucleases (9,63). However, coupling siRNA or DNA to HGN using thiol-gold conjugation chemistry (Fig. 7) provides high surface concentrations so that hundreds to thousands of molecules are delivered by a single HGN conjugate (9,10,63–65). Tightly packed RNA or DNA on the gold surface is protected from enzyme degradation (63,64) and the innate immune response to densely, oligonucleotide-functionalized gold nanoparticles is ~ 25 times less than a lipoplex carrying the same DNA (64). The effect is due to the inhibition of

proteins recognizing foreign nucleic acids by the steric hindrance and high charge density of the densely bound DNA or RNA.

However, for the siRNA and other payloads to function, they must be rapidly and completely released from the HGN on command. Relatively low intensity pulses of NIR light can induce sufficient surface temperature changes in the HGN that gold-thiol bonds are broken, releasing siRNA from the HGN quickly and efficiently, without damaging the siRNA, DNA, or small molecules (9,10,66,67). Only the irradiated HGN release their payload, providing a means of controlling release from the HGN in both space and time. An important feature of pulsed NIR light delivery is that the nucleic acid payload is released within seconds. This is quite different than schemes to raise the temperature of the nanoparticles with low intensity, continuous irradiation to induce DNA or RNA dehybridization, which takes hours of continuous NIR light exposure for only partial release (63,68,69).

Unfortunately for efficient transfection, even if targeted cells take up nanoparticles, the carrier and its load are sequestered within endocytic vesicles and may be transported to lysosomes, eliminated, or destroyed (Figs. 7, 8) (9,10,68,70–72). Endosome escape is the most difficult to overcome bottleneck for drug and synthetic oligonucleotide delivery (9,10,70,71). Materials such as siRNA that function within the cytoplasm are prevented from reaching the site of action, which can often only be addressed by using significantly higher concentrations to insure that sufficient active material escapes to the cytoplasm (62). Chemical disruptors such as photosensitizers (often initiated with cytotoxic, poorly penetrating UV light) (70), polymers that change volume with temperature shock (72), or pH via the “proton sponge” effect (71), have been used to release cargo from endosomes, but with low efficiency and increased toxicity. Such disruptors are often incompatible with living organisms and like Lipofectamine, cannot be used in vivo.

However, HGN-induced microbubble formation (as in Figure 6) induced by pulsed NIR light of the appropriate intensity can generate sufficient mechanical forces that the endosome is disrupted, without otherwise damaging the cell or the material within the endosome (See Fig. 7,8) (9,10). This allows the contents of the endosome to mix with the cytoplasm. A distinct energy threshold is required to disrupt the endosome that is greater than that necessary to release the thiol bonds holding the siRNA to the HGN (9). The energy threshold for endosome rupture is similar to that found to disrupt lipid vesicles that contain HGN (4,5,9). Photomechanical endosome rupture requires no new chemical species such as photochemical degradation products (70) or high ion concentrations (71) to be introduced into the cell. Transfection occurs only after NIR light-triggered endosome disruption, with efficiencies as good or better than Lipofectamine (Invitrogen. Carlesbad, CA), the current “gold” standard for transfection *in vitro* (9). However, unlike Lipofectamine, HGN-siRNA conjugates can be introduced into the circulation and have been shown to promote gene silencing in HeLa tumors in mice (10) after laser irradiation.

Figure 7B shows TEM images of the intracellular distribution of HGN with and without NIR irradiation. Nude mice bearing HeLa cervical cancer xenografts injected with HGN showed that the HGN were located in endocytic vesicles (endosomes and lysosomes) (10) with intact membranes before laser irradiation. However, after laser irradiation, the boundaries of the endocytic vesicle membranes appeared disrupted, resulting in the escape of nanoparticles from the endosomes into the cytosol.

Figure 8 shows cultured mouse epithelial cells expressing green fluorescent protein (C166-GFP), which were transfected with HGN thiol-linked to a siRNA construct labeled with red Cy3 dye (9). The RNA sequence was based off the EGFP-S1 Dicer Substrate, previously

shown to potently silence GFP, and modified with necessary PEG thiol, amino, and Cy3 modifications, leaving the antisense 3' unmodified for Dicer activity (9). The attached Cy3 made visualization of the release of the RNA sequence from the HGN possible; the dye was partially quenched when near gold, and dequenches upon release from the HGN. Low intensity laser pulses could disrupt the bonds between the HGN and the siRNa, resulting in increased Cy3 fluorescence due to the increased separation between the nanoshells and dye (Fig. 8a). However, the red Cy3 fluorescence remained localized within endosomes as small, bright red, puncta (Fig. 8a) and there was little silencing of the GFP. As in Fig. 7, this shows that the HGN are localized within endosomes after transfection into cells.

Higher intensity NIR light pulses (Fig. 8b) ruptured the endosomes, likely by mechanical forces due to microbubble formation (Fig. 6), releasing the siRNA to the cytosol. By controlling the light intensity, endosomes could be ruptured without damaging the cells or the siRNA. Within 24 hours of the second pulse, the Cy3 fluorescence was diffuse, indicating release from the endosomes (Fig. 7b). This release was accompanied by near-complete silencing of the GFP in cells irradiated by NIR light. The GFP levels were determined by pixel intensities to be essentially equal, 80% silenced for laser exposed NS-siRNA and 85% for Lipofectamine (Invitrogen. Carlesbad, CA), relative to controls. Negative control HGN composed of 2'Ace-protected sense strand hybridized to antisense DNA-Cy3, prepared identically to the NS-siRNA, exhibited no silencing activity after laser exposure. Furthermore, laser exposure of wells containing only cells indicated no photobleaching of GFP.

Unlike other viral or non-viral delivery vectors, HGN-induced gene delivery can be spatially controlled. Payloads are released and endosomes ruptured only where the sample is irradiated; gene silencing can be patterned using lithography or by focusing the light through a microscope. Fig. 8c shows that a simple mask can be used to pattern GFP silencing with near single-cell resolution. siRNA release and endosome rupture can be separated in time, as the energy requirements for the two processes are different. Low intensity light pulses below threshold can dissociate the thiol bonds used to link molecules to the HGN, while intensity above the threshold disrupts the endosomes. Even higher light intensities can be used to kill cells outright through thermal ablation (59), or in synergy with drug stresses. Although the HGN temperature increase is substantial, the temperature increase in the sample is < 1° C. Cell toxicity is minimal and is less than Lipofectamine (Invitrogen. Carlesbad, CA).

4. Future Prospects

Liposomes remain immensely appealing as a drug delivery platform; endosomes, lysosomes, synaptic vesicles, etc. show that nature has taken full advantage of their properties to enhance the localization and transport *in vivo*. However, unilamellar liposome may be too simple a structure to achieve the myriad requirements of a universal drug carrier. Unfortunately, each added layer of complexity increases the difficulty of commercial scale-up; targeting, enhanced drug retention, drug release rate control, extended time in the circulation must be done in as simple and synergistic fashion possible, while retaining the innate biocompatibility that makes liposomes so appealing. Dividing these jobs between multiple membranes and add-ons such as gold nanoparticles may make it possible to develop a modular and commercially viable drug delivery system in the future. The goal of the colloid scientist is to present the oncologist of the future with the ability to choose specific drug release rates, the times and places of drug release, and a minimum of side effects from inappropriate release of drug to non-targeted tissues. The long sought, "magic bullet" for drug delivery may still be a liposome.

Acknowledgments

This work was supported by NIH Grants HL080718 and EB012637. The author thanks M. Sailor, D. Lapotko, C. Li and F. Caruso for the generous use of their figures in this review.

References and Suggested Reading

1. Chandrawati R, Hosta-Rigau L, Vanderstraaten D, Lokuliyana Sa, Stadler B, Albericio F, Caruso F. Engineeering advanced capsosomes: maximizing the number of subcompartments, cargo retention, and temperature triggered reaction. ACS Nano. 2010; 4:1351–1361. [PubMed: 20192233] This paper describes the construction and properties of a liposome/polymer composite structure made by layer by layer self-assembly.
2. Boyer C, Zasadzinski JA. Multiple lipid compartments slow vesicle contents release in lipases and serum. ACS Nano. 2007; 1:176–182. [PubMed: 18797512] Multiple lipid shells, even if they are of the same composition, dramatically enhance drug retention in serum.
3. Bolinger PY, Stamou D, Vogel H. An integrated self-assembled nanofluidic system for controlled biological chemistries. Angew Chem Int Ed. 2008; 47:5544–5549.
4. Wu G, Mikhailovsky A, Khant HA, Fu C, Chiu W, Zasadzinski JA. Remotely Triggered Liposome Release by Near-Infrared Light Absorption via Hollow Gold Nanoshells. Journal of the American Chemical Society. 2008; 130:8175–8177. [PubMed: 18543914]
5. Wu GH, Mikhailovsky A, Khant HA, Zasadzinski JA. Synthesis, characterization and optical response of gold nanoshells used to trigger release from liposomes. Meth Enzymology. 2009; 464:279–295.Liposomes can be rapidly ruptured and their contents released by conjugation to surface plasmon resonant gold nanoparticles after exposure to near infrared light.
6. Park J-H, von Maltzahn G, Xu MJ, Fogal V, Kotamraju VR, Ruoslahti E, Bhatia SN, Sailor MJ. Cooperative nanomaterial system to sensitize, target and treat tumors. Proc Natl Acad Sci USA. 2010; 107:981–986. [PubMed: 20080556] Up-regulation of receptors via NIR heating of nanorods improved efficacy of targeted liposomes.
7. Troutman TS, Leung SJ, Romanowski M. Light-induced content release from plasmon-resonant liposomes. Advanced Materials. 2009; 21:2334–2340.
8. Anderson LJE, Hansen E, Lukianova-Hleb EY, Hafner JH, Lapotko DO. Optically guided controlled release from liposomes with tunable plasmonic nanobubbles. J Controlled Release. 2010; 144:151–158.Direct images of micron sized vapor bubbles generated by pulsed laser heating of gold nanoparticles.
9. Braun GB, Pallaoro A, Wu GH, Missirlis D, Zasadzinski JA, Tirrell M, Reich NO. Laser-activated gene silencing via gold nanoshell-siRNA complexes. ACS Nano. 2009; 3:2007–2015. [PubMed: 19527019] Gold nanoshells can selectively release thiol-linked siRNA and rupture endosomes depending on NIR light intensity to induce green fluorescence protein silencing in living cells.
10. Lu W, Zhang G, Zhang R, Flores LGI, Huang Q, Gelovani JG, Li C. Tumor site-specific sliencing of NF-kB p65 by targeted hollow gold nanosphere-mediated photothermal transfection. Cancer Research. 2010; 70:3177–3188. [PubMed: 20388791] First in vivo demonstration of siRNa transfection using NIR light induced endosome release.
11. Phillips MA, Gran ML, Peppas NA. Targeted nanodelivery of drugs and diagnostics. Nanotoday. 2010; 5:143–159. [PubMed: 20543895]
12. Sugahara KN, Teesalu T, Karmali P, Kotamraju VR, Agemy L, Greenwald DR, Ruoslahti E. Coadministration of a tumor-penetrating peptide enhances the efficacy of cancer drugs. Science. 2010; 328:1031–1035. [PubMed: 20378772] Peptide makes solid tumors permeable to nanocarriers.
13. Moen MD, Lyseng-Williamson KA, Scott LJ. Liposomal amphotericin BP a review of its use as empirical therapy in febrile neutropenia and in the treatment of invasive fungal infections. Drugs. 2009; 69:361–392. [PubMed: 19275278]
14. Spector MS, Zasadzinski JA, Sankaram MB. Topology of multivesicular liposomes. Langmuir. 1996; 12:1196–1199.
15. Peer D, Karp JM, Hong S, Farokhzad OC, Margalit R, Langer R. Nanocarriers as an emerging platform for cancer therapy. Nature Nanotechnology. 2007; 2:751–760.

16. Ruoslahti E, Bhatia SN, Sailor MJ. Targeting of drugs and nanoparticles to tumors. J Chem Biol. 2010; 188:759–768.

17. Choi HS, Liu W, Misra P, Tanaka E, Zimmer JP, Ipe BI, Bawendi MG, Frangioni JV. Renal clearance of quantum dots. Nature Biotechnology. 2007; 25:1165–1170.

18. Hambley TW, Hait WN. Is anticancer drug development heading in the right direction? Cancer Res. 2009; 69:1259–1262. [PubMed: 19208831]

19. Pastorino F, Di Paolo D, PIccardi F, Nico B, Ribatti D, Daga A, Baio G, Neumaier CE, Brignole C, Loi M, Marimpietri D, Pagnan G, Cilli M, Lepenkhin EA, Garde SV, Longhi R, Corti A, Allen TM, Wu JJ, Ponzoni M. Enhanced antitumor efficacy of clinical-grade vasculature-targeted liposomal doxorubicin. Clin Cancer Res. 2008; 14:7320–7329. [PubMed: 19010847]

20. Champion JA, Mitragotri S. Shape induced inhibition of phagocytocis of polymer particles. Pharmaceutical Res. 2009; 26:244–249.Macrophage phagocytocis depends on the shape and size of materials.

21. Dos Santos N, Allen C, Doppen AM, Anantha M, Cox KAK, Gallagher RC, Karlsson G, Edwards K, Kenner G, Samuels L, Webb MS, Bally MB. Influence of poly(ethylene glycol) grafting density and polymer length on liposomes: relating plasma circulation lifetimes to protein binding. Biochimica et Biophyisca Acta. 2007; 1768:1367–1377.Suggests that the role of PEG is primarily to prevent liposome aggregation rather than opsonization.

22. Moghimi SM, Hamad I. Liposome mediated triggering of complement cascade. J Liposome Research. 2008; 18:195–209. [PubMed: 18720195] Mechanisms of liposome-induced immune response leading to clearance

23. Hamad I, Al-Hanbali O, Hunter AC, Rutt KJ, Andresen TL, Moghimi SM. Distinct polymer architecture mediates switching of complement activation pathways at the nanosphere-serum interface: implications for stealth nanoparticle engineering. ACS Nano. 2010; 4:6630–6638.Density of PEG packing determines immune response to nanoparticles

24. Leal C, Rognvaldsson S, Fossheim S, Nilssen EA, Topgaard D. Dynamic and structural aspects of PEGylated liposomes monitored by NMR. J Colloid Interfac Sci. 2008; 325:485–493.PEG-lipids induce changes in liposome structure and can exchange with bulk solution

25. Lindner LH, Eichhorn ME, Eibl H, Teichert N, Schmitt-Sody M, Issels RD, Dellian M. Novel temperature-sensitive liposomes with prolonged circulation time. Clin Cancer Res. 2004; 10:2168–2178. [PubMed: 15041738] Short, hydrogen bonding headgroups can lead to enhance circulation by increasing hydrophilicity of liposome surfaces

26. Barauskas J, Cervin C, Jankunec M, Spandyreva M, Ribokaite K, Tiberg F, Johnsson M. Interactions of lipid-based liquid crystalline nanoparticles with model and cell membranes. Int J Pharm. 2010; 391:284–291. [PubMed: 20214966]

27. You J, Shao R, Wei X, Gupta S, Li C. Near-infrared light triggers release of paclitaxel from biodegradable microspheres: photothermal effect and enhanced tumor activity. Small. 2010; 6:1022–1031. [PubMed: 20394071]

28. Abraham SA, Waterhouse DN, Mayer LD, Cullis PR, Madden TD, Bally MB. The liposomal formulation of doxorubicin. Methods in Enzymology. 2005; 391:71–97. [PubMed: 15721375]

29. Noble CO, Guo Z, Hayes ME, Marks JD, Park JW, Benz CC, Kirpotin DB, Drummond DC. Characterization of highly stable liposomal and immunoliposomal formulations of vincristine and vinblastine. Cancer Chemother Pharmacol. 2009; 64:741–751. [PubMed: 19184019]

30. Drummond DC, Noble CO, Hayes ME, Park JW, Kirpotin DB. Pharmacokinetics and In Vivo drug release rates in liposomal nanocarrier development. J Pharm Sci. 2008; 97:4696–4740. [PubMed: 18351638]

31. Volodkin DV, Skirtach AG, Mohwald H. Near IR remote release from assemblies of liposomes and nanoparticles. Angew Chem Int Ed. 2009; 48:1807–1809.

32. Senior J, Gregoriadis G. Stability of small unilamellar liposomes in serum and clearance from the circulations: the effects of the phospholipid and cholesterol components. Life Sciences. 1982; 30:2123–2136. [PubMed: 7109841]

33. Johnston MJW, Semple SC, Klimuk SK, Ansell S, Maurer N, Cullis PR. Characterization of the drug retention and pharmacokineic properties of liposomal nanoparticles containing dihydrosphingomyelin. Biochimica et Biophyisca Acta. 2007; 1768:1121–1127.

34. Huang Z, Jaafari MR, Szoka FC. Disterolphospholipids: nonexchangeable lipids and their application to liposomal drug delivery. Angew Chem Int Ed. 2009; 48:4146–4149.
35. Huang S-L. Liposomes in ultrasonic drug and gene delivery. Advanced Drug Delivery Reviews. 2008; 60:1167–1176. [PubMed: 18479776]
36. Rothblat GH, Phillips MC. High-density lipoprotein heterogeneity and funciton in reverse cholesterol transport. Current Opinion in Lipidology. 2010; 21:229–238. [PubMed: 20480549] Cholesterol exchange mechanisms can destabilize liposomes in vivo
37. Phillips MC, Johnson WJ, Rothblat GH. Mechanisms and consequences of cellular cholesterol exchange and transfer. Biochimica et Biophyisca Acta. 1987; 906:223–276.
38. Coldren BA, Warriner HE, van Zanten R, Zasadzinski JA, Sirota E. Zero spontaneous curvature and its effects on lamellar phase morphology and vesicle size distributions. Langmuir. 2006; 22:2472–2481.
39. Wang B, Zhang L, Bae SC, Granick S. Nanoparticle-induced surface reconstruction of phospholipid membranes. Proc Natl Acad Sci U S A. 2008; 105:18171–18175. [PubMed: 19011086]
40. Yu Y, Granick S. Pearling of lipid vesicles induced by nanoparticles. J Am Chem Soc. 2009:14158–14159. [PubMed: 19775107] Interactions between liposomes and nanoparticles can induce significant changes in liposome structure and shape.
41. Le Bihan O, Bonnafous P, Marak L, Bickel T, Trepout S, Mornet S, De Haas F, Talbot H, Taveau JC, Lambert O. Cryo-electron tomography of nanoparticle transmigration into liposome. J Structural Biol. 2009; 168:419–425.
42. Jin Y, Gao X. Spectrally tunable leakage-free gold nanocontainers. J Am Chem Soc. 2009; 131:17774–17775. [PubMed: 19928855]
43. Prevo BG, Esakoff SA, Mikhailovsky A, Zasadzinski JA. Scalable routes to gold nanoshells with tunable sizes and properties: monitoring their response to NIR pulsed laser irradiation. Small. 2008; 4:1183–1195. [PubMed: 18623295]
44. Zasadzinski JA, Bailey SM. Applications of Freeze-Fracture Replication to Problems in Materials and Colloid Science. J Electron Microsc Technique. 1989; 13:309–334.
45. Fukui Y, Fujimoto K. The preparation of sugar polymer-coated nanocapsules by the layer-by-layer deposition on the liposome. Langmuir. 2009; 25:10020–10025. [PubMed: 19705896]
46. Johnston APR, Such GK, Caruso F. Triggering release of encapsulated cargo. Angew Chem Int Ed. 2010; 49:2664–2666.
47. Wong B, Boyer C, Steinbeck C, Peters D, Schmidt J, van Zanten R, Chmelka B, Zasadzinski JA. Design and in situ characterization of lipid containers with enhanced drug retention. Advanced Materials. 2011 in press.
48. Minchinton AI, Tannock IF. Drug penetration in solid tumors. Nature Rev Cancer. 2006; 6:583–592. [PubMed: 16862189]
49. Tredan O, Galmarini CM, Patel K, Tannock IF. Drug resistance and the solid tumor microenvironment. J Natl Cancer Inst. 2007; 99:1441–1454. [PubMed: 17895480]
50. Huang XH, Neretina S, El-Sayed MA. Gold nanorods: from synthesis and properties to biological and biomedical applications. Adv Materials. 2010; 21:4880–4910.
51. Hossan M, Wang T, Wiggenhorn M, Schmiidt R, Zengerle A, Winter G, Eibl H, Peller M, Reiser M, Issels RD, Lindner LH. Size of thermosensitve liposomes influences content release. J Controlled Release. 2010; 147:436–443.
52. Huang S-L, MacDonald RC. Acoustically active liposomes for drug encapsulation and ultrasound-triggered release. Biochimica et Biophysica Acta, Biomembranes. 2004; 1665:134–141.
53. Shum P, Kim J-M, Thompson DH. Phototriggering of liposomal drug delivery systems. Advanced Drug Delivery Reviews. 2001; 53:273–284. [PubMed: 11744172]
54. Mueller A, Bondurant B, O'Brien DF. Visible-Light-Stimulated Destabilization of PEG-Liposomes. Macromolecules. 2000; 33:4799–4804.
55. Ponce AM, Vujaskovic Z, Yuan F, Needham D, Dewhirst MW. Hyperthermia mediated liposomal drug delivery. Int J Hyperthermia. 2006; 22:205–213. [PubMed: 16754340] Review of the effects of hyperthermia on cancer treatment with temperature sensitive liposomes.

56. Davidsen J, Jorgensen K, Andresen TL, Mouritsen OG. Secreted phospholipase A(2) as a new enzymatic trigger mechanism for localised liposomal drug release and absorption in diseased tissue. Biochimica et Biophyisca Acta. 2003; 1609:95–101.
57. Morton JG, Day ES, Halas NJ, West JL. Nanoshells for photothermal cancer therapy. MethodsMol Biol. 2010; 624:101–117.Review of the development of surface plasmon resonant nanoshells and their use in medicine.
58. Chen J, Wang D, Xi J, Au L, Siekkinen A, Warsen A, Li Z-Y, Zhang H, Xia Y, Li X. Immuno Gold Nanocages with Tailored Optical Properties for Targeted Photothermal Destruction of Cancer Cells. Nano Lett. 2007; 7:1318–1322. [PubMed: 17430005]
59. Jain PK, Huang XH, El-Sayed IH, El-Sayed MA. Noble metals on the nanoscale: optical and photothermal properties and some applications in imaging, sensing, biology and medicine. Acc Chem Res. 2008; 41:1578–1586. [PubMed: 18447366]
60. Skrabalak SE, Chen JY, Sun YG, Lu X, Au L, Cobley LM, Xia YN. Gold nanocages: synthesis, properties and applications. Acc Chem Res. 2008; 41:1587–1595. [PubMed: 18570442]
61. Lukianova-Hleb EY, Hu Y, Latterini L, Tarpani L, Lee SY, Drezek RA, Hafner JH, Lapatko DO. Plasmonic nanobubbles as transient vapor nanobubbles generated around plasmonic nanoparticles. ACS Nano. 2010; 4:2109–2123. [PubMed: 20307085] Rapid heating of nanoparticles results in formation of vapor bubbles
62. Giljohann DA, Seferos DS, Prigodich AE, Patel PC, Mirkin CA. Gene regulation with polyvalent siRNA - nanoparticle conjugates. J Am Chem Soc. 2009; 131:2072–2073. [PubMed: 19170493]
63. Barhoumi A, Huschka R, Bardhan R, Knight MW, Halas NJ. Light-induced release of DNA from plasmon-resonant nanoparticles: towards light-controlled gene therapy. Chem Phys Letters. 2009; 482:171–179.
64. Massich MD, Giljohann DA, Seferos DS, Ludlow LE, Horvath CM, Mirkin CA. Regulating immune response using polymalent nucleic acid-gold nanoparticle conjugates. Molecular Pharmaceutics. 2009; 6:1934–1940. [PubMed: 19810673]
65. Prabaharan M, Grailer JJ, Pilla S, Steeber DA, Gong S. Gold nanoparticles with a monolayer of doxorubicin-conjugated amphiphilic block copolymer for tumor-targeted drug delivery. Biomaterials. 2009; 30:6065–6075. [PubMed: 19674777]
66. Jain PK, Qian W, El-Sayed MA. Ultrafast cooling of photoexcited electrons in gold nanoparticle-thiolated DNA conjugates involves the dissociation of the gold-thiol bond. J Am Chem Soc. 2006; 128:2426–2433. [PubMed: 16478198] Pulsed NIR light induces thiol bond cleavage from gold nanoparticle without damage to the rest of the tethered molecule.
67. Wijaya A, Schaffer SB, Paliares IG, Hamad-Schifferli K. Selective release of multiple DNA oligonucleotides from gold nanorods. ACS Nano. 2009; 3:80–86. [PubMed: 19206252]
68. Lee SE, Liu GL, Kim F, Lee LP. Remote optical switch for localized and selective control of gene interference. Nano Lett. 2009; 9:562–570. [PubMed: 19128006]
69. Jones MR, Millstone JE, Giljohann DA, Seferos DS, Young KL, Mirkin CA. Plasmonically controlled nucleic acid dehybridization with gold nanoprisms. Chem Phys Chem. 2009; 10:1461–1465. [PubMed: 19431161]
70. de Bruin KG, Fella C, Ogris M, Wagner E, Ruthardt N, Brachle C. Dynamics of photoinduced endosomal release of polyplexes. J Controlled Release. 2008; 130:175–182.
71. Mintzer MA, Simanek EE. Nonviral vectors for gene delivery. Chem Rev. 2009; 109:259–302. [PubMed: 19053809]
72. Lee SH, Choi SH, Kim SH, Park TG. Thermally sensitive cationic polymer nanocapsules for specific cytosolic delivery and efficient gene silencing of siRNa: swelling induced disruption of endosomes by cold shock. J Controlled Release. 2008; 125:25–32.

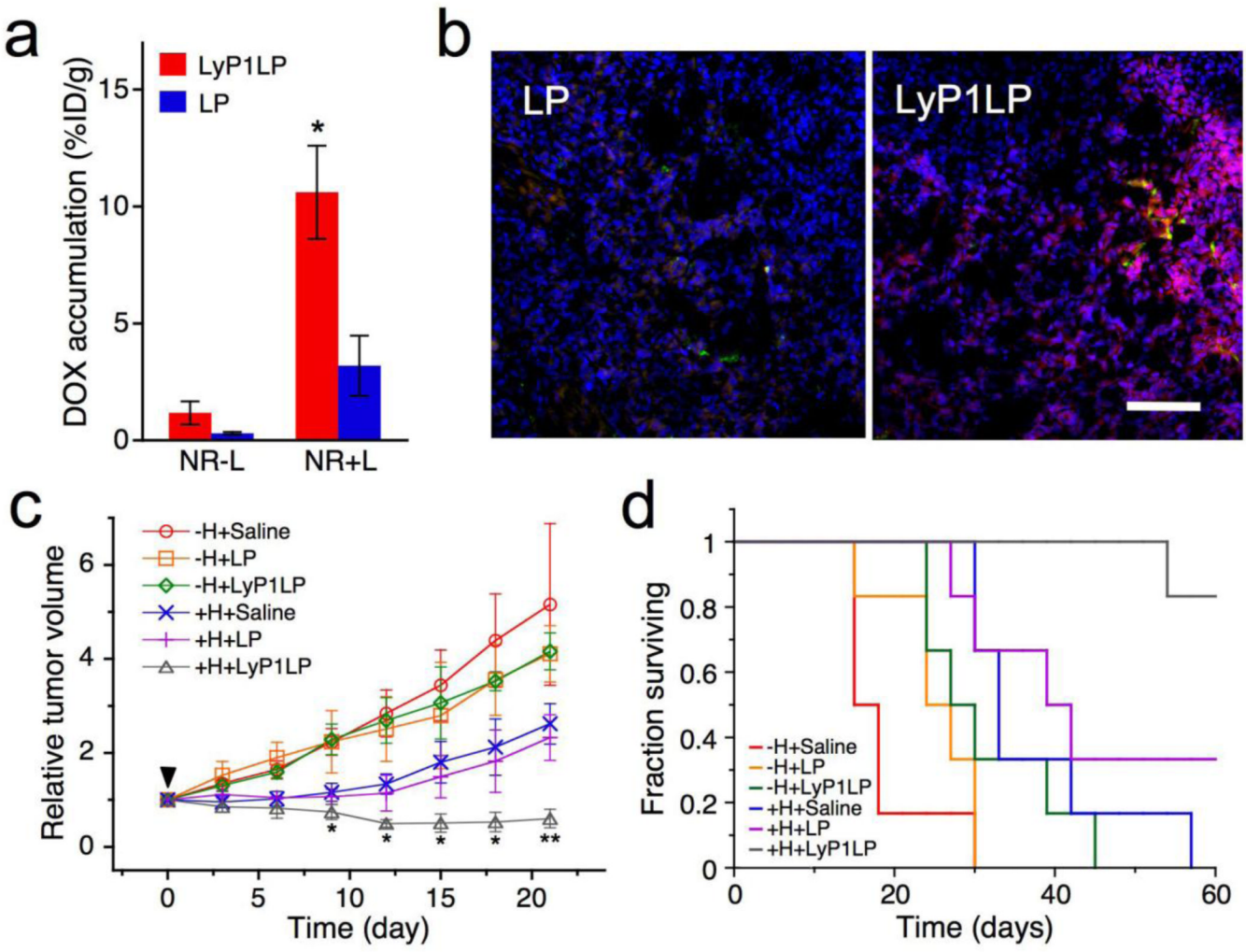

Figure 1.

Enhanced antitumor therapy using near infrared light-heated gold nanorods to up-regulate specific receptors in mice bearing MDA-MB-435 tumors, which are then targeted by a specific ligand on liposomes that contain dox (LyP1LP). **(A)** Relative accumulation of dox in tumor for targeted (red) vs untargeted (blue) liposomes without heating (NR−L) or with heating (NR+L) to upregulate the receptor. **(B)** Increased levels of dox (red) are observed in tumors from the mice in (A) subjected to heating (NR+L) when treated with liposomes with (LyP1LP) campared to those without (LP) ligand. Nanoparticles are dyed green; cell nuclei are stained blue. Scale bar is 100 microns. **(C)** Change in tumor volume of different treatment groups containing bilateral MDA-MB-435 xenograft tumors. 72 hours post-injection of gold nanorods, mice were injected with a single dose of saline, untargeted liposomes (LP) and targeted liposomes (LyP1LP). +H designates one of the two tumors in each animal that was heated. −H designates the tumor that was not heated. **(D)** Survival rate in different treatment groups after a single 3 mg Dox/kg dose into mice containing a single tumor. Adapted and reproduced with permission from NAS from Figure 4 of Park et al. Proc Natl Acad Sci USA. 2010;107:981–6 (6).

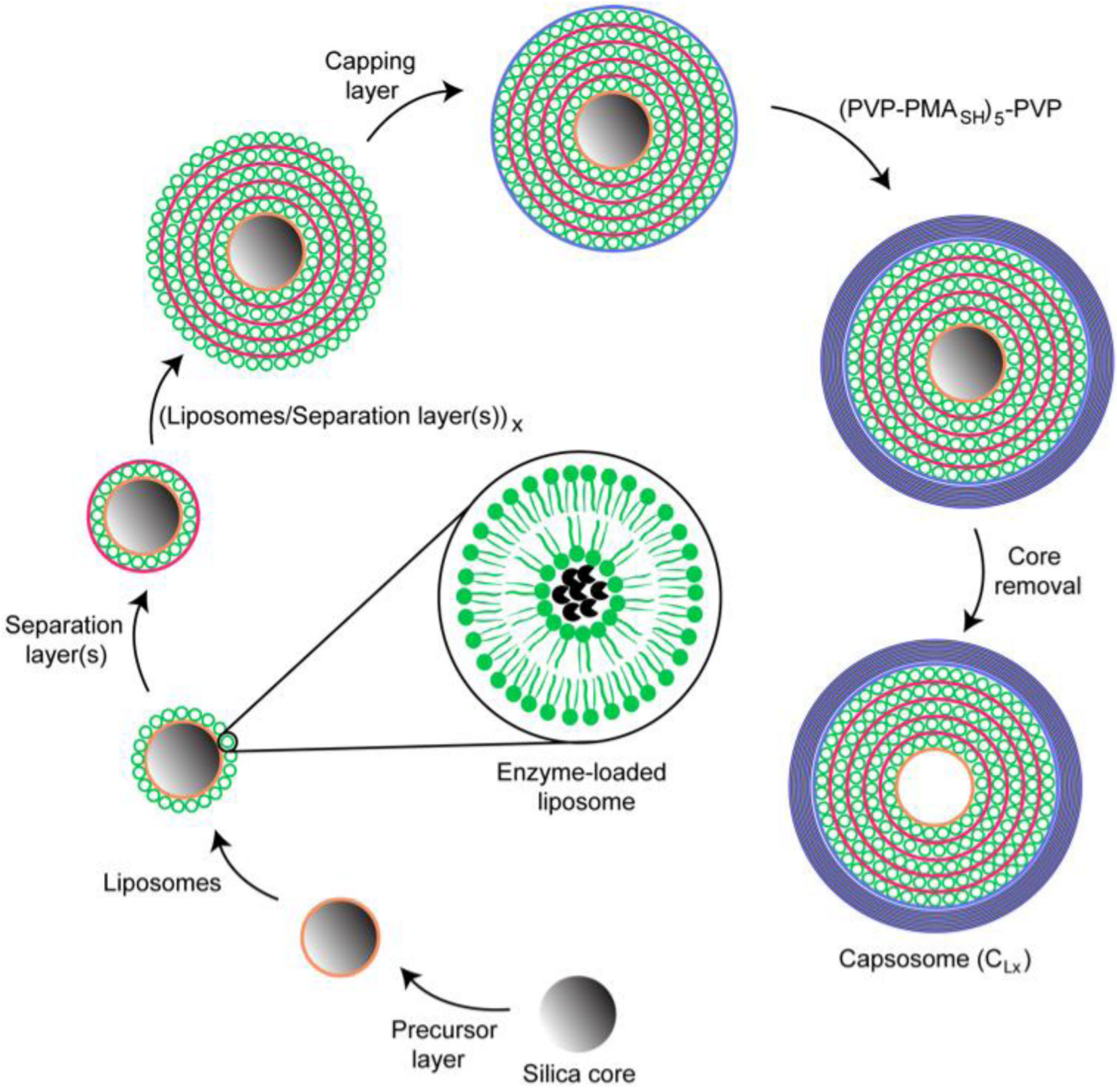

Figure 2.

Schematic illustration of “capasome” self-assembly process. An anionic silica core (3 micron diameter) is coated with a cationic polymer precursor layer, followed by a layer of anionic liposomes. This can be followed by the alternating deposition of separation layers and liposomes until the desired number of liposome layers is reached. A polymer capping layer is adsorbed prior to the deposition of five bilayers of PVP and PMA_{SH}. The capping layer is crosslinked to stabilize the structure. Dissolution of the core results in a caposome with multiple layers of intact liposomes. Adapted and reproduced with permission from ACS from Scheme 1 of Chandrawati et al. ACS Nano. 2010;4:1351–61 (1).

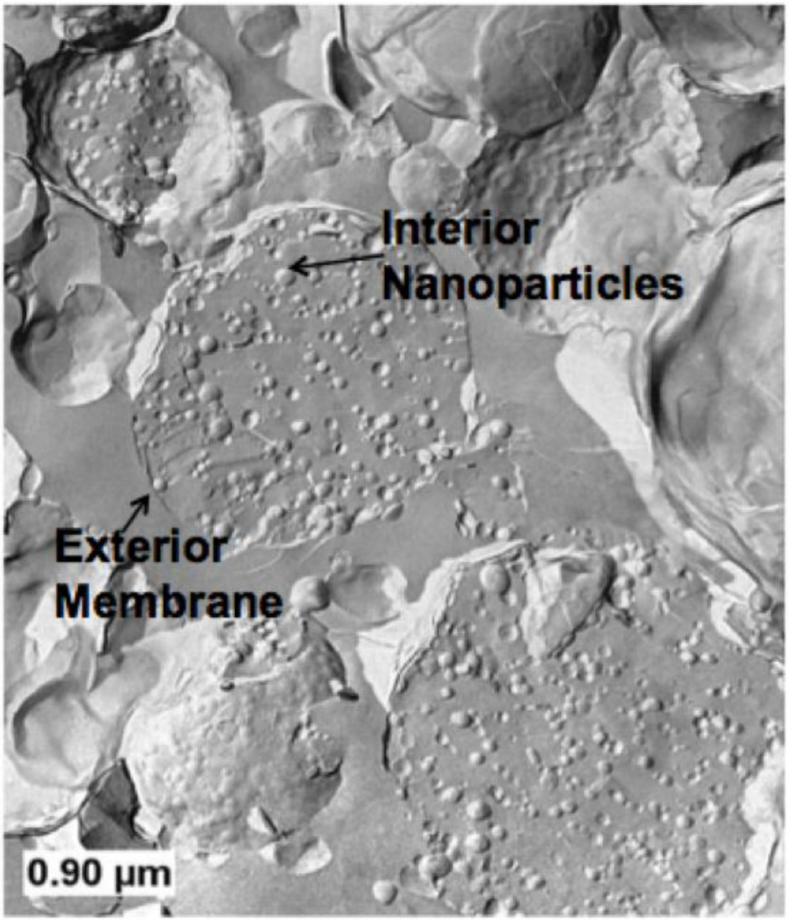

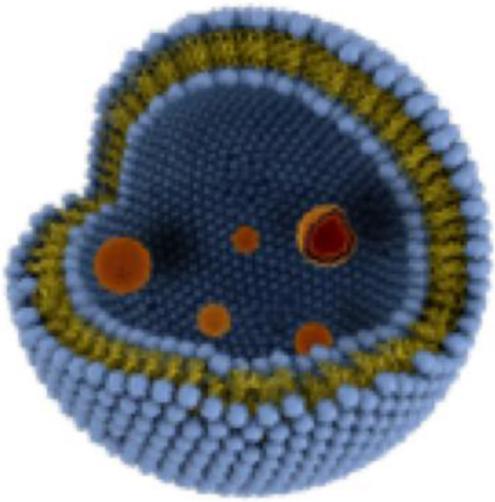

Figure 3.
Schematic (right) and freeze-fracture transmission electron micrograph (left) of vesosome structure. Small, unilamellar vesicles (50 – 100 nm diameter) are encapsulated within 200 – 2000 nm diameter bilayers formed by the transition from the interdigitated L_{bI} phase to the L_a phase induced by heating the sample above 45° C. Here the interior and exterior compartments are both made of dipalmitoylphosphatidylcholine.

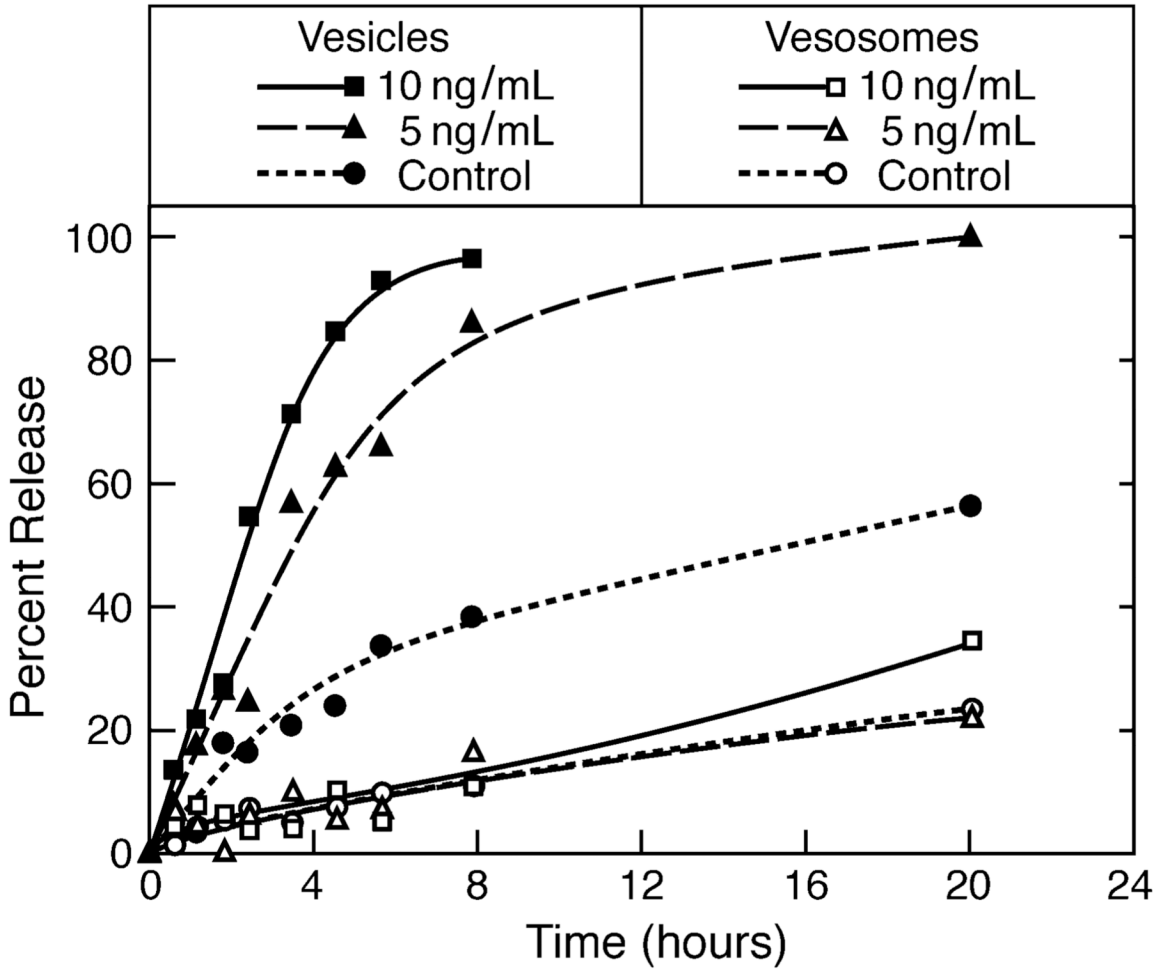

4a.

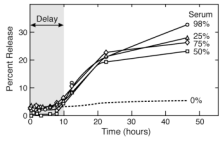

4b.

Figure 4.

(a) Comparison of dye release from unilamellar vesicles and vesosomes of DPPC on exposure to varying amounts of porcine pancreas phospholipase A_2 at 37° C. PLA_2 induces rapid release from unilamellar DPPC vesicles in a concentration dependent manner (closed

symbols), causing complete dye release within 4– 8 hours. Essentially no release beyond background is induced by PLA_2 from vesosomes (open symbols) suggesting that the PLA_2 cannot reach the interior compartments of the vesosome where the dye is sequestered. Adapted and reproduced with permission from ACS from Figure 2 of Boyer et al. ACS Nano. 2007;1:176–82 (2). **(b)** Dye release from the DPPC within DPPC vesosome has a distinct delay (about 10 hours) during which almost nothing is released. Even in 98% serum, there is only 30% release in 50 hours. Unilamellar DPPC vesicles are completely empty after 2 hours exposure to serum. The exterior membrane protects the interior compartments from the degradation due to the various components of serum such as the HDL and lipases. Adapted and reproduced with permission from ACS from Figure 5 of Boyer et al. ACS Nano. 2007;1:176–82 (2).

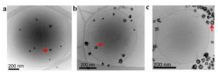

Figure 5.

(a) Cryo-TEM image of unilamellar DPPC liposome encapsulating hollow gold nanoshells (HGN, arrows). The nanoshells were encapsulated using the same interdigitated sheet method used to make the vesosome. (b) HGN tethered to the vesicle using a thiol-PEG-lipid linker (arrow) (c) HGN mixed with liposomes. Pulsed laser irradiation causes microbubble formation that can disrupt the liposomes within seconds (Fig. 6); the closer the nanoshells are to the liposome membrane, the greater the efficiency of drug release. Adapted and reproduced with permission from ACS from Figure 1 of Wu et al. J. American Chemical Society. 2008;130:8175–7 (4).

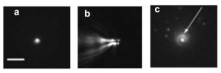

Figure 6.

An individual 80% dioleoylphospholcholine (DOPC), 20% dioleoyl trimethylammonium propane (DOTAP) liposome containing fluorescent allophycocyanin (APC) protein and 80 nm gold nanoparticles (NPs) attached to an anionic glass surface before light irradiation. **(b)** 10 nsec after irradiation, optical scattering from a vapor bubble generated from heat dissipation from the nanoparticle as it cooled. Note the anisotropy of the bubble (pulse length 0.5 ns, wavelength 532 nm (c) 10 msec after irradiation, the APC fluorescence has expanded (arrow), signifying ejection from liposome. (Scale bar is 10 μm. Adapted and reproduced with permission from Elsevier from Figure 4 of Anderson et al. J. Controlled Release. 2010;144:151–8. (8).

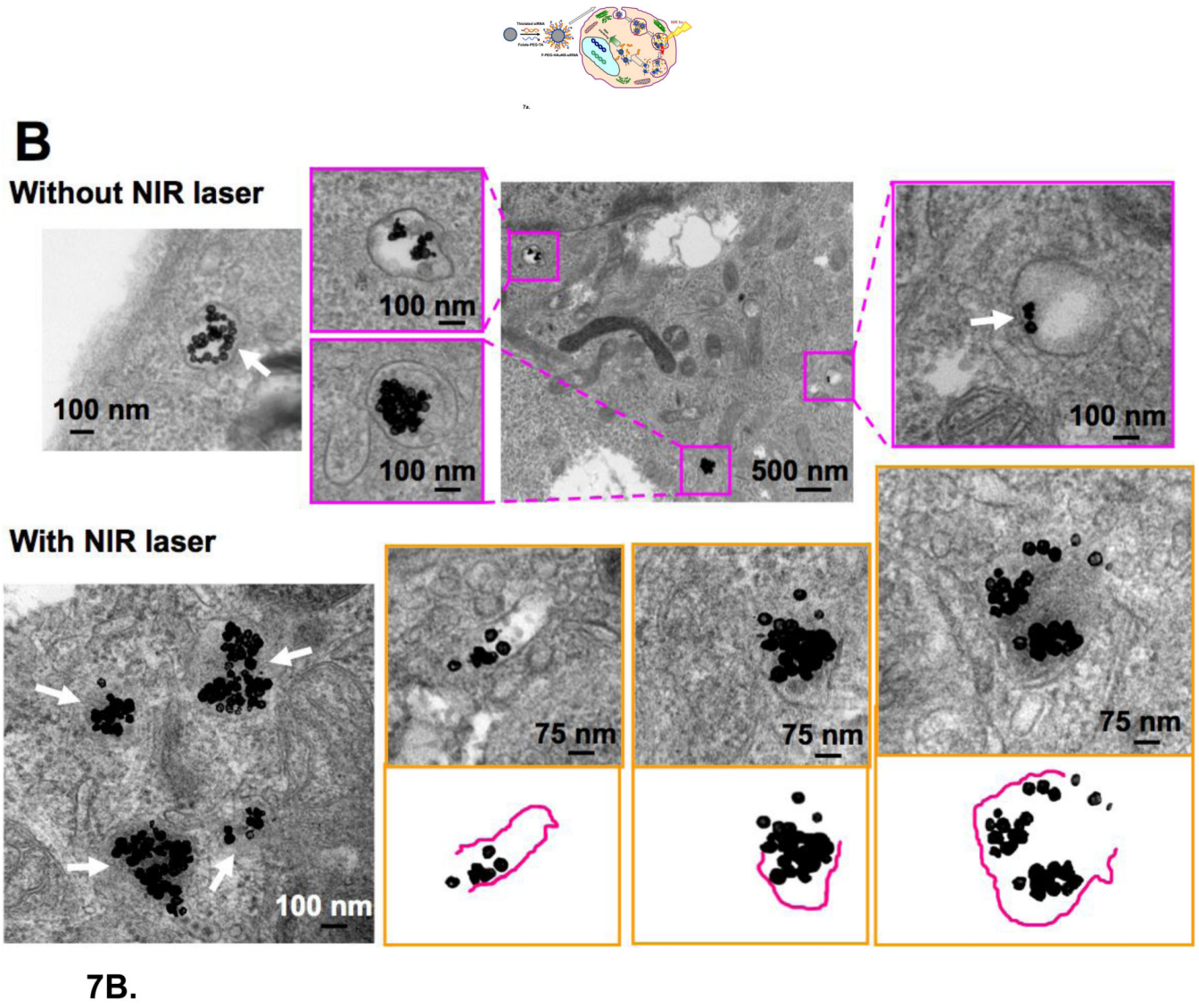

7B.

Figure 7.

(a) Schematic diagram of siRNA delivery vector based on hollow gold nanoshells and disrupting endosome membranes in living cells. Thiolated siRNA is coupled to the HGN to compact and protect the siRNA from degradation and deliver thousands of oligonucleotides with each nanoparticle. Thiolated PEG with targeting peptides can be used to stabilize the HGN against aggregation and target specific internalizing receptors on cells. Once the HGN-siRNA conjugate is internalized within a cell, usually within an endosome, pulsed NIR light of the appropriate intensity can be used to release the siRNA by first cleaving the thiol bonds to the gold, followed by a higher intensity pulse to disrupt the endosome membrane in the same way liposome membranes are disrupted though the formation of microbubbles (Fig. 6). The intact siRNA is released to the cell cytoplasm which allows for siRNA silencing of protein function. **(b)** Transmission electron micrographs of intracellular distribution of folate-labelled gold nanoshells, thiol linked to siRNA, without (top) or with (bottom) NIR pulsed laser irradiation. Arrow in the top left and top right panels indicate that prior to irradiation the HGN remain attached to the rim of endocytic vesicles. Arrows in the bottom left panel show that the endocytic vesicle membranes have been disrupted by the

NIR irradiation. Higher magnification images with schematics show that some parts of the endocytic vesicles have disappeared, resulting in endolysosomal escape of the HGN to the cytosol. Adapted and reproduced with permission from AACR from Figure 2 of Lu et al. Cancer Research. 2010;70:3177–88 (10).

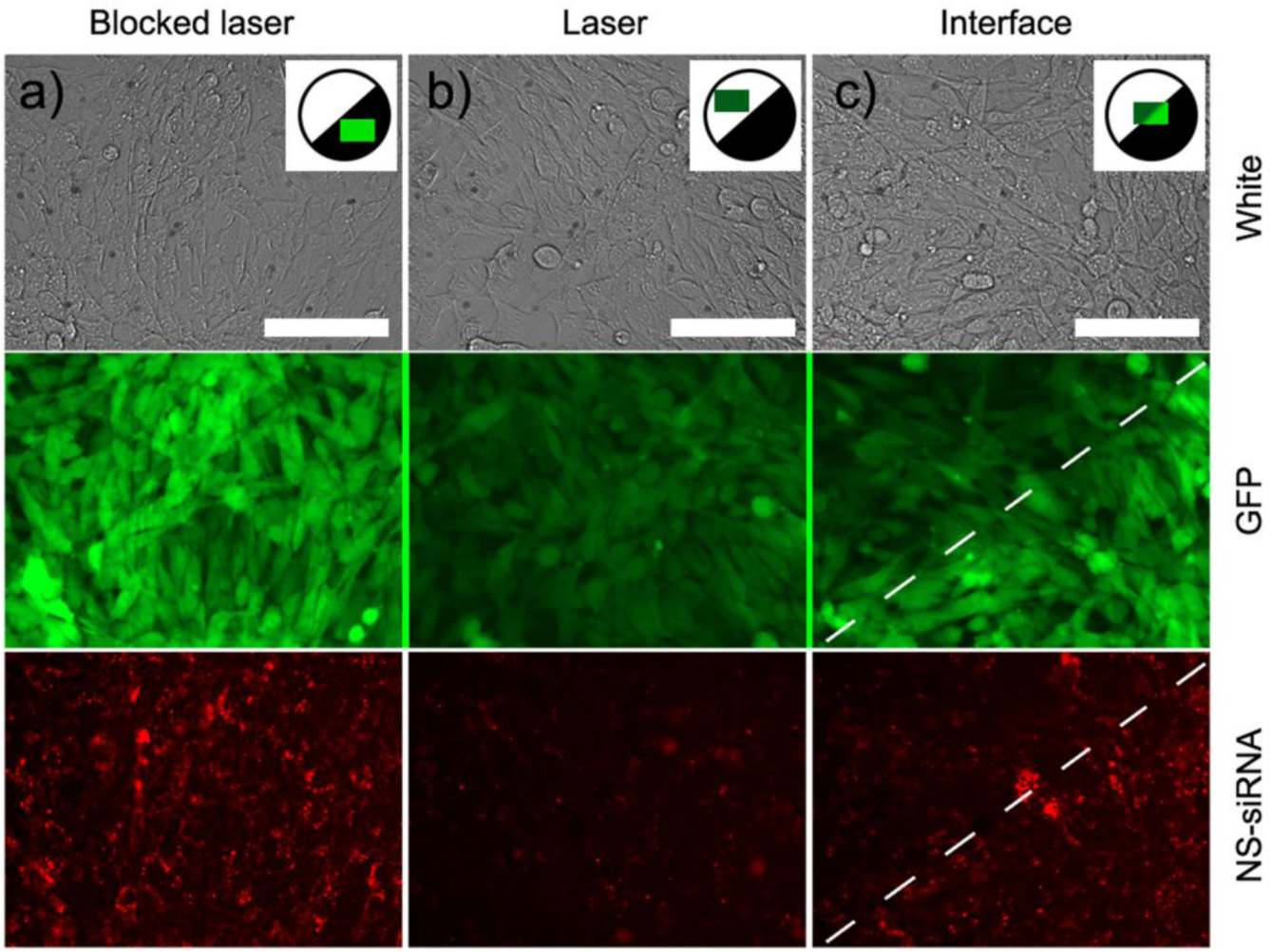

Figure 8.

Patterned exposure by blocking one half of the femtosecond pulsed NIR laser beam illuminating 5 mm diameter wells containing mouse epithelial cells expressing green fluorescent protein (GFP). Cells were previously exposed to Tat-lipid labeled HGN thiol-coupled to siRNA (See Fig. 7a). The siRNA was labeled with Cy3 (red) dye which is dequenched when released from the nanoshells by low intensity NIR light. Images were taken ~ 32 hours after NIR irradiation. **(a)** Cells and HGN-siRNA in a region blocked by the mask shows high GFP. The Cy3 dye is localized to small bright puncta, consistent with entrapment within intact endosomes. **b)** In NIR light-exposed cells, there is a 90% drop in GFP expression and the red Cy3 has diffused throughout the cells, with fewer puncta, indicating the disruption of the endosomes and transport of the siRNA to the cytosol, allowing the GFP to be silenced. **c)** Imaging the interface between exposed and unexposed regions shows the spatial control possible with HGN induced transfection. The white dashed line indicates the border of knockdown, which corresponds to the pattern edge. GFP and red puncta of the Cy3 are visible in the unexposed regions, while in the exposed regions, the Cy3 is diffuse and the GFP is silenced. The resolution is about 1 cell diameter. Scale bars 50 μm. Adapted and reproduced with permission from ACS from Figure 5 of Braun et al. ACS Nano. 2009;3:2007–2015 (9).